

Article

A Novel Polishing Method for Extending the Service Life of Magnetic Compound Fluid

Youliang Wang ^{1,*}, Xichun Gao ¹, Jibo Gao ¹, Xiujuan Chen ¹, Wenjuan Zhang ² and Ming Feng ³¹ School of Mechanical and Electrical Engineering, Lanzhou University of Technology, Lanzhou 730050, China² State Key Laboratory of Advanced Processing and Recycling of Nonferrous Metals, Lanzhou University of Technology, Lanzhou 730050, China³ College of Mechanical and Electrical Engineering, Wenzhou University, Wenzhou 325035, China

* Correspondence: wangyouliang20@lut.edu.cn

Abstract: Magnetic field-assisted magnetic compound fluid (MCF) ultra-precision machining technology is regarded as an effective method to obtain a smooth surface. However, due to the evaporation and splashing of water in the polishing fluid during processing, the service life of the MCF slurry is reduced. This paper presents a material removal model for MCF polishing, and a novel experimental apparatus is proposed to extend the service life by supplying MCF components into the MCF slurry. Firstly, in order to obtain the ideal polishing tool, the appearance morphologies and the formation process of the MCF slurry were observed by an industrial camera. On this basis, the optimum parameters were determined by multi-factor and multi-level orthogonal experiments. Finally, the investigation of the MCF service life was carried out under the optimal processing parameters. The main findings are summarized as follows. (1) Excellent MCF polishing tools are obtained when the eccentric distance r is 4 mm and the MCF slurry supply V is 1 mL. (2) When the eccentric distance increases from 2 mm to 4 mm, the forming time of the MCF tool decreases sharply, but when the eccentricity exceeds 4 mm, the decreasing trend becomes slow. The molding time grows steadily as the supply is increased. (3) When the machining gap Δ , the MCF carrier speed n_c , the eccentricity r , and the revolution speed of magnetic n_m are 1 mm, 500 rpm, 4 mm, and 600 rpm, respectively, the ideal machining effect can be obtained. (4) It could be proven that the polishing device is feasible to extend the service time of the MCF slurry by adding MCF components.

Keywords: magnetic compound fluid; polishing; surface roughness; material removal; service life



Citation: Wang, Y.; Gao, X.; Gao, J.; Chen, X.; Zhang, W.; Feng, M. A Novel Polishing Method for Extending the Service Life of Magnetic Compound Fluid.

Lubricants **2022**, *10*, 299. <https://doi.org/10.3390/lubricants10110299>

Received: 29 September 2022

Accepted: 4 November 2022

Published: 6 November 2022

Publisher's Note: MDPI stays neutral with regard to jurisdictional claims in published maps and institutional affiliations.



Copyright: © 2022 by the authors. Licensee MDPI, Basel, Switzerland. This article is an open access article distributed under the terms and conditions of the Creative Commons Attribution (CC BY) license (<https://creativecommons.org/licenses/by/4.0/>).

1. Introduction

With the rapid development of aerospace, biomedical, electronics, new energy, and other industries, the requirements for ultra-smooth optical components increases. Therefore, the effect of grinding technology has attracted a lot of attention. The conventional grinding techniques usually remove the material with rigid polishing tools [1–3]. Although good surface roughness can be obtained, it has disadvantages, such as low form accuracy, uncontrollable material removal, and the easy production of a subsurface damage layer during polishing [4]. Hence, it is difficult to obtain reliable ultra-smooth optical components through conventional grinding techniques [5,6].

In order to obtain optical components with smooth surfaces, researchers have made a variety of attempts. Previous studies have found that it is difficult to effectively enhance the surface quality of optical components when only relying on the improvement and adjustment of tools, machines, and process parameters. In this case, energy field-assisted processing methods, including magnetic field-assisted polishing, electrophoresis polishing, ultrasonic vibration polishing, chemical mechanical polishing, etc., have become a relevant issue in the research of finishing technology [7]. These processing methods are characterized by using energy fields such as magnetic fields, electric fields, ultrasonic fields, and chemical

fields as auxiliary means to obtain high surface quality indirectly or directly [8,9]. Compared with other energy field auxiliary processing methods, it involves a low cost, a wider application range, and a simple polishing device. Magnetic field-assisted polishing is a promising and effective machining method for obtaining high surface quality [10].

Magnetic field-assisted polishing is widely used in the machining of optical components and semiconductors with high precision and high surface quality [11,12], and it has no subsurface damage and good controllability in the machining process. Compared with other polishing methods, magnetic field-assisted polishing has lower costs, simpler polishing devices, and a wider application range. It is a promising and effective machining method to obtain high surface quality. Tani et al. [13] proposed the technology of magnetic fluid (MF) finishing. The abrasive grains were blended into the magnetic fluid, and the micro-cutting effect of the abrasive grains in the magnetic fluid was controlled by the magnetic field to remove the material. A smooth acrylic resin was obtained with a roughness of less than 0.04 μm . The particle dispersion of MF is stable, but its viscosity and magnetic pressure are so low that the polishing force of the abrasive grain is weak [14]. Therefore, MF is widely used in damping, lubrication, sensors, and biomedicine [15]. Kordonski et al. [16] presented a magnetorheological (MR) finishing technique, which works by exploiting the unique fluidity of magnetorheological fluid in a magnetic field. Magnetorheological polishing technology is widely studied because of its low surface roughness and high material removal rate (MRR). It is often used to process aspheric surfaces, inner tube walls, and hard, brittle materials [17,18]. Jha et al. [19–21] combined the advantages of abrasive flow machining with the advantages of magnetorheological finishing and developed magnetorheological abrasive flow finishing, which can achieve internal complex geometry processing to nano-precision. Zhang et al. [22,23] developed ultrasonic magnetorheological compound finishing (UMC), which overcame the difficulty of processing the small concave surface and free-form surface with MR finishing. The surface roughness after processing can be lower than Ra 3.5 nm. However, compared with MF slurry, the particle distribution in MR fluid slurry is unstable, which makes it difficult to stabilize its surface treatment performance [24].

In order to address the disadvantages of MF and MR fluids, a new type of magnetic slurry, called magnetic composite fluid (MCF) slurry, was proposed [25]. MCF is made by mechanically mixing micron carbonyl iron powder (CIP), α -cellulose fibers, and abrasive grains with MF containing nano-magnetic particles. MCF slurry combines the advantages of MR and MF fluids. Hence, the polishing fluid shows higher viscosity, magnetic pressure, and more stable particle dispersion. At the same time, MCF slurry maintains excellent fluidity [26,27]. Based on the outstanding properties of MCF, a new contact-free polishing tool using MCF slurry was developed by Shimada et al., and mirror processing on the rib-shaped groove of a brass specimen was successfully realized [28]. Through the study of Shimada et al., the process parameters of contact-free MCF slurry polishing were optimized by Furuya and Wu et al. Furuya et al. [29] processed stainless steel (SUS304), explained the influence of different mixing ratios of iron powder and non-magnetic abrasive grains on the polishing characteristics, and expounded the polishing performance under different external magnetic fields. Wu et al. [30] verified the influence of the process parameters on the polishing characteristics by using MCF slurry to polish acrylic resin. Nevertheless, the magnetic line of force and flux density remain constant in the static magnetic field. The external conditions determine the shape and spatial position of magnetic clusters in MCF slurry. In addition, the abrasive grains are wrapped in magnetic collections, which hinders the uniform distribution of the abrasive grains. These behaviors are not conducive to the surface finishing of the workpiece. In fact, the shape recovery ability of MCF slurry under a static magnetic field is very weak [31]. Therefore, Sato et al. [32] decided to use a dynamic magnetic field and keep the magnetic flux density of the field constant so that the magnetic field line would continue to rotate as the magnet position changed. Previous studies have shown that the polishing effect of MCF slurry is better in a dynamic magnetic field than in a static magnetic field. Although the dynamic magnetic field weakens the

initial polishing force slightly, the non-magnetic abrasive grains are more evenly distributed in the dynamic magnetic field, which improves the shape recovery ability of the MCF slurry. Thus, MCF slurry can have good polishing force and improve the polishing performance during polishing [33].

Although many studies have proven that the magnetic field-assisted MCF polishing technology can obtain a higher-quality surface, the MCF carrier plate will change the viscosity of the MCF slurry during processing and rotation, thus accelerating the loss of water in the polishing solution (evaporation and splash), and ultimately significantly affecting the polishing performance of the MCF slurry. Therefore, the MCF slurry needs to be replaced frequently to ensure the polishing quality, which leads to a large increase in time costs and processing costs [34]. Hence, ensuring the usage time of MCF slurry in the polishing process has become a key problem in the research of MCF slurry.

2. Experimental Details

2.1. Polishing Principle

To ensure the service life of MCF slurry, a new processing method for MCF using an injector to add MCF components regularly was proposed. Figure 1 shows the principle of MCF polishing. The cylindrical magnet is installed on the left side of the bracket; the eccentricity r is adjusted by moving the magnet and is driven by a servo motor with coupling. The MCF slurry carrier plate is installed in front of the cylindrical magnet with a clearance of δ , which is driven by another servo motor through a belt. When the cylindrical magnet rotates around the spindle and the main shaft, it will produce a dynamic magnetic field of constant strength. The rotating speed of the magnetic field is n_m , and its magnetic induction line changes regularly with the rotation of the magnet. At the same time, in order to prevent non-magnetic abrasive grains from staying in the same place for a long time during processing, the MCF carrier plate is rotated at a speed n_c . A certain amount of MCF polishing solution is attached to the bottom of the liquid carrier plate. The nano-magnetic particles and micron carbonyl iron powder in the polishing solution are distributed along the magnetic induction line under the action of the dynamic magnetic field to form a chain structure, and these chain structures form magnetic clusters. Afterward, the viscoelasticity of the magnetic collections is enhanced by the α -cellulose fibers interspersed between magnetic clusters. Most of the abrasive grains are concentrated around the apex of the magnetic cluster due to the magnetic levitation force, and these particles are trapped in the magnetic cluster or distributed among carbonyl iron powder particles. Finally, in order to maintain the abrasive grains, a polishing tool that can restore the appearance is formed. When the polishing tool is used to process the parts, the abrasive grains in the polishing fluid act on the surface of the machined workpiece, and the micro-cutting effect produced by the abrasive grains is used to remove materials. After processing for a while, we use a syringe to add a certain volume of MCF components to the MCF slurry to extend the usage time of MCF slurry. The MCF components are rapidly blended with the MCF slurry due to the stimulating effect generated by the constant rotation of the magnetic line of force. Thus, the polishing performance of the MCF slurry is maintained.

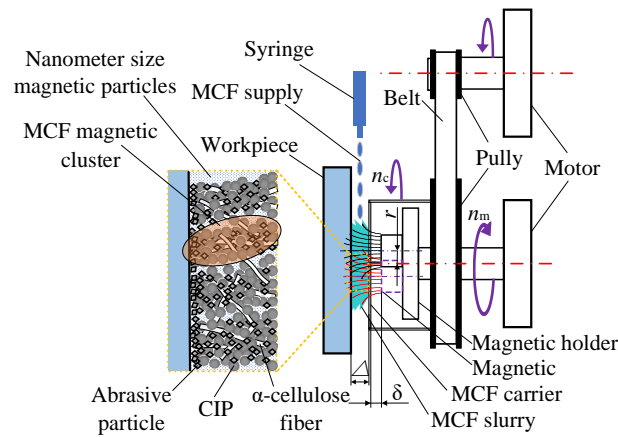


Figure 1. Polishing principle of magnetic compound fluid (MCF) polishing process.

According to previous research, a non-magnetic abrasive moves from a high-magnetic-field area to a low-magnetic-field area under the effect of the magnetic suspension force [35,36]. Therefore, the forces of abrasive grains are mainly magnetic levitation force and gravity, and gravity does not affect the polishing process. Based on the theoretical analysis of Sidpara et al., the magnetic levitation force F_{abr} of wear particles is given as [37,38]

$$F_{abr} = V_{abr}\mu_0 M_f \nabla H \tag{1}$$

where V_{abr} is the volume of abrasive grains, μ_0 is the permeability of a vacuum, M_f is the intensity of magnetization of the MCF slurry, and ∇H is the gradient of the magnetic field, which is related to the machining gap Δ .

Assuming that the magnetic particles in the MCF slurry are spherical, the intensity of magnetization M of the magnetic particles is [39]

$$M = \frac{3(\mu - \mu_0)}{\mu + 2\mu_0} H \tag{2}$$

where μ is the permeability of the magnetic particle, and H is the magnetic field intensity. If the volume ratio of magnetic particles in MCF slurry is φ , the magnetization intensity of MCF slurry M_f can be expressed as [40]

$$M_f = \varphi M \tag{3}$$

A typical material removal mechanism is shown in Figure 2 [41]. The abrasive grains are pressed into the machined surface of the workpiece under the action of magnetic levitation force. The abrasive grains are moved due to the MCF fluid plate rotation. With the increase in processing time, some peaks are removed, and the surface roughness is decreased.

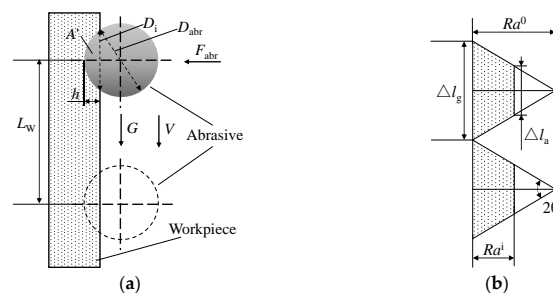


Figure 2. Material removal mechanism: (a) schematic diagram of material removal mechanism, (b) simplified surface geometry.

The indentation diameter of the abrasive grains pressed into the material can be determined by the hardness of the material. The Brinell hardness H_B is calculated by the following formula

$$H_B = \frac{2F_{abr}}{\pi D_{abr} \left(D_{abr} - \sqrt{D_{abr}^2 - D_i^2} \right)} \quad (4)$$

where D_{abr} is the diameter of the abrasive grain, and D_i is the indentation diameter of the abrasive grain pressed into the material.

Thus, the indentation diameter D_i can be expressed as

$$D_i = \sqrt{\frac{4F_{abr}}{\pi H_B} - \frac{4F_{abr}^2}{(\pi D_{abr} H_B)^2}} \quad (5)$$

Therefore, the projected area of indentation S_i is

$$S_i = \pi \left(\frac{D_i}{2} \right)^2 = \frac{\pi F_{abr} D_{abr}^2 H_B - F_{abr}^2}{\pi (D_{abr} H_B)^2} \quad (6)$$

According to the classical dynamics, the relative velocity of abrasive grains and workpiece surface V can be expressed as

$$V = \frac{2\pi R n_c}{60} \quad (7)$$

where R is the radius of the point where the abrasive grains are located in the polishing area, which is related to the eccentricity r , and n_c is the rotational speed of the MCF fluid carrier plate.

The pressure P of the abrasive grain on the surface is

$$P = \frac{F_{abr}}{S_i} \quad (8)$$

The Preston equation is generally used to express the relationship between the material removal rate and processing parameters. The Preston equation can be described as

$$MRR = KP V \quad (9)$$

where K is the empirically determined Preston coefficient.

According to the theory of the Preston equation, the material removal rate of a single abrasive grain in MCF polishing is expressed as

$$MRR = \frac{k R n_c \pi^2 D_{abr}^2 H_B^2}{30 \pi D_{abr}^2 H_B - 90 \varphi V_{abr} H \nabla H \frac{\mu_0(\mu - \mu_0)}{\mu + 2\mu_0}} \quad (10)$$

The workpiece surface has irregular bumps with a random distribution. To determine the surface roughness machining model, it is assumed that the workpiece has a uniform roughness profile that is triangular, as shown in Figure 2b. Ra^0 is the initial surface roughness before polishing, and Ra^i is the surface roughness after a stroke (a stroke is defined as a circle of abrasive grains around the center of the polishing area). The actual contact length L_a between the abrasive grains and the work surface is proportional to the moving distance L_w of the abrasive grains, and the expression is as follows [42]:

$$L_a = \left(\frac{\Delta l_a}{\Delta l_w} \right) L_w = \left[\frac{(Ra^0 - Ra^i) \tan \theta}{Ra^0 \tan \theta} \right] L_w = \left(1 - \frac{Ra^i}{Ra^0} \right) L_w \quad (11)$$

The depth h of the workpiece surface embedded with abrasive grains is

$$h = \frac{D_{abr}}{2} - \frac{1}{2} \sqrt{D_{abr}^2 - D_i^2} \quad (12)$$

The area of the abrasive grains pressed into the surface of the workpiece A' is

$$A' = \frac{D_{abr}^2}{4} \sin^{-1} \left[\frac{2\sqrt{h(D_{abr}-h)}}{D_{abr}} \right] - \sqrt{h(D_{abr}-h)} \left(\frac{D_{abr}}{2} - h \right) \quad (13)$$

According to the research of Jain et al., the indentation volume of abrasive grains on the workpiece surface can be defined as material removal [43]. Hence, the material removal of a single abrasive grain in the i th stroke can also be expressed as the product of the actual contact length between the abrasive grain and the surface and the cross-sectional area of the abrasive grain embedded in the surface.

$$MR_i = A' L_a = \left\{ \frac{D_g^2}{4} \sin^{-1} \left[\frac{2\sqrt{h(D_g-h)}}{D_g} \right] - \sqrt{h(D_g-h)} \left(\frac{D_g}{2} - h \right) \right\} \left(1 - \frac{Ra^i}{Ra^0} \right) L_w \quad (14)$$

The total volume of material removed after n times of cutting is

$$MR = \sum_{i=1}^n MR_i = \left\{ \frac{D_{abr}^2}{4} \sin^{-1} \left[\frac{2\sqrt{h(D_{abr}-h)}}{D_{abr}} \right] - \sqrt{h(D_{abr}-h)} \left(\frac{D_{abr}}{2} - h \right) \right\} L_w \sum_{i=1}^n \left(1 - \frac{Ra^i}{Ra^0} \right) \quad (15)$$

Comparing Equations (10) and (15), the surface roughness model can be simplified as follows:

$$Ra^n = nRa^0 - \frac{Ra^0 MRR \cdot t}{A' L_w} - \sum_{i=1}^{n-1} Ra^i \quad (16)$$

Thus, the final surface quality is closely related to the polishing time, the initial roughness, and the MRR, while the MRR is related to the machining gap, the speed, and the eccentricity of the MCF carrier. Therefore, we need to pay attention to the machining gap, the MCF carrier plate speed, and the influence of eccentricity on the polishing performance. In addition, the rotational speed of magnets can irritate the MCF slurry, so the influence of the rotation speed of the magnet on the polishing performance should be considered.

2.2. Experimental Setup

To achieve the processing principle, the experimental setup shown in Figure 3 was constructed in the laboratory based on a three-way milling machine. The polishing unit is composed of a non-magnetic MCF carrier and a servo motor, which drives the rotation of the MCF carrier through a belt. A cylindrical magnet (φ 20 mm \times t 10 mm, 0.5 T) that can adjust the eccentricity distance is installed on the front side of the magnet bracket, and the rotation of the magnet base is controlled by another motor. The workpiece is fixed on the Z-axis of the three-way milling machine, and the position of the workpiece is adjusted by moving the X-axis and Z-axis. The workpiece is located in the front side of the MCF liquid carrier plate, leaving a certain machining gap. Therefore, the machining gap of the workpiece can be adjusted instantly by controlling the three-way milling machine. Because the magnet has a certain eccentric distance from the magnet base axis, the dynamic magnetic field will be generated when the magnet base rotates.

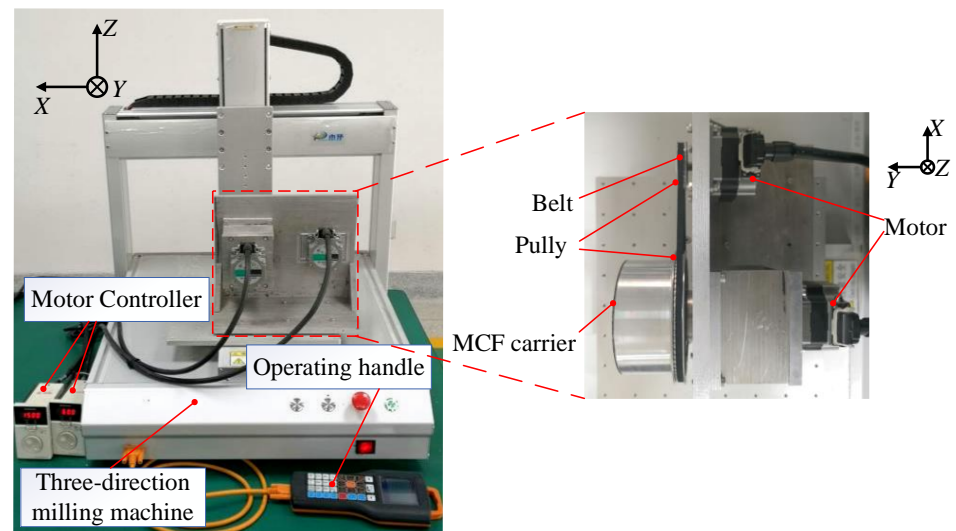


Figure 3. A photograph of the constructed setup.

2.3. Experimental Conditions and Procedures

To show the polishing effect of this new device in more detail, there are two steps in this experiment. Firstly, the forming process and final morphology of the MCF cutter were observed under different experimental conditions to obtain the appropriate cutter. In the second step, the optimal parameters of the experimental setup were determined through orthogonal experiments. Furthermore, the influences of the given polishing parameters on the surface quality were analyzed. Finally, the service life of the MCF slurry was studied under the optimal processing parameters.

The MCF slurry compositions and its distribution are shown in Table 1. The optimum composition of MCF of 45 wt.% water-based magnetic fluid, 40 wt.% iron powder, 12 wt.% abrasive grains, and 3 wt.% α -cellulose was chosen firstly, according to the previous study. Table 2 shows the process parameters of this experiment. A polycarbonate board (PC board) was chosen as the workpiece to explore the polishing characteristics of the proposed experimental installation and effectively extend the service life of the MCF slurry. In addition, 800-mesh sandpaper was used to polish the workpiece surface so that the roughness of the workpiece surface was approximately 500 nm.

Table 1. Compositions of MCF slurries used.

Water-based magnetic fluid (MF)	mean diameter	10 nm
	concentration	45 wt.%
Carbonyl iron powder (CIP)	mean diameter	7 μ m
	concentration	40 wt.%
Abrasive grain (Al_2O_3)	mean diameter	1 μ m
	concentration	12 wt.%
α -cellulose	concentration	3 wt.%

Table 2. Experimental conditions.

Parameters	Value
Workpiece	Polycarbonate board: L 50 mm \times W 50 mm \times t 1 mm Φ 20 mm \times t 10 mm
Permanent magnet	B = 0.5 T $r = 2, 4, 6, 8$ mm
MCF carrier	$n_m = 300, 400, 500, 600$ rpm
Supplying of MCF slurry, V	$n_c = 200, 300, 400, 500$ rpm
Machining gap, Δ	1, 1.5, 2, 2.5 mL
Processing time, t	1, 1.5, 2, 2.5 mm 10 min

3. Results and Discussion

3.1. MCF Tool

The polishing performance of slurry is profoundly influenced by the appearance of MCF during the polishing process; therefore, it is necessary to observe the size of MCF appearance and its formation process in order to obtain a suitable MCF slurry.

The observation process of MCF slurry is shown in Figure 4. Initially, a certain volume of MCF polishing solution is adsorbed on the side surface of the MCF carrier plate through a syringe. Afterward, under the action of an external magnetic field, the MCF slurry is stably adsorbed on the MCF carrier plate. Subsequently, the permanent magnet rotates with the magnetic holder at a speed of $n_m = 600$ rpm, and the MCF carrier also rotates at a speed of $n_c = 500$ rpm in the opposite direction. The MCF slurry with the initial state varies with polishing time, and finally forms a complete MCF polishing tool. An industrial camera (OSG130-210UM by YVISION) was used to observe the formation process with various eccentricity values and MCF supply to reveal the formation time. Finally, the cross-section of the MCF tool was measured to obtain the size of its appearance morphology using an optical photograph.

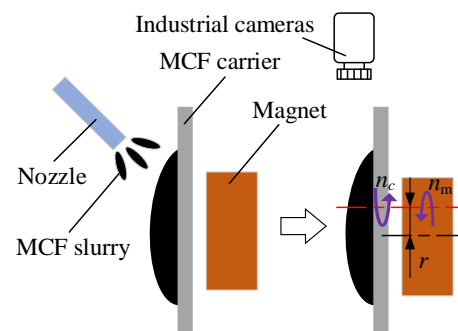


Figure 4. Illustration of MCF tool formation process observation.

The formation process of a typical MCF tool under magnet eccentricity $r = 4$ mm and MCF supply $V = 1$ mL is shown in Figure 5. The poor appearance of the MCF tool was observed in the initial state (0 ms) when the MCF slurry was only injected into the MCF carrier. Once the motor drives the magnet and the magnet seat to rotate around the spindle, the morphology of the MCF slurry will immediately change with the magnet. Eventually, a complete MCF slurry is formed at $t = 950$ ms, which was better than previous research conclusions [44]. Moreover, it should be noted that the formation time T of the MCF slurry can be defined as the period from the initial state to the formation of an extremely regular appearance of the MCF slurry.

To further explore the polishing performance of the MCF slurry, the sizes of the MCF tool's appearance shape were quantitatively studied. The final appearances of MCF tools with different eccentricities and MCF supplies are displayed in Figures 6 and 7, respectively. It can be found that the effect of eccentricity on the MCF appearance is greater than that of the MCF supply. The bulky magnetic clusters can be notably observed when the eccentricity is smaller than 4 mm, which indicates that the MCF slurry was stirred insufficiently. Once the eccentricity is larger than 4 mm, the magnetic clusters are vimineous and uniform. With the amount of MCF slurry supply increasing, the height and diameter of the MCF tool increase.

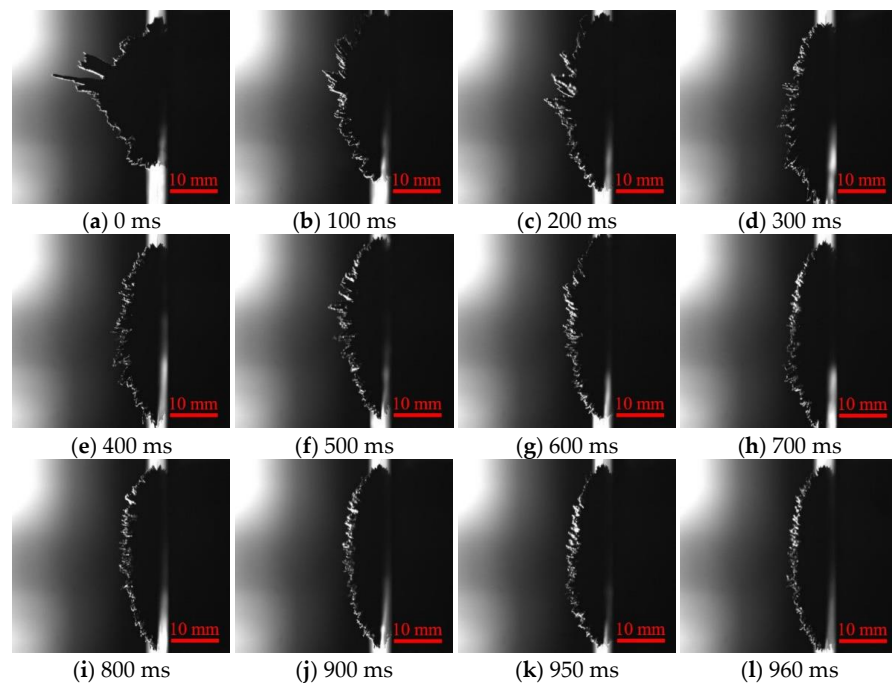


Figure 5. The formation process of a typical MCF slurry under magnet eccentricity $r = 4$ mm and MCF supply $V = 1$ mL.

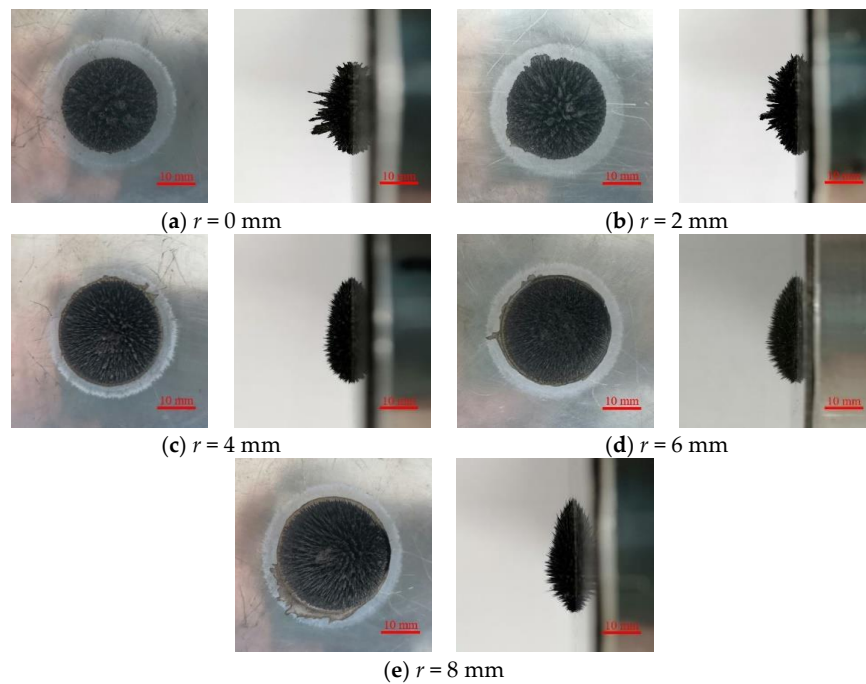


Figure 6. The final appearances of MCF tools with different eccentricities under MCF supply of 1 mL.

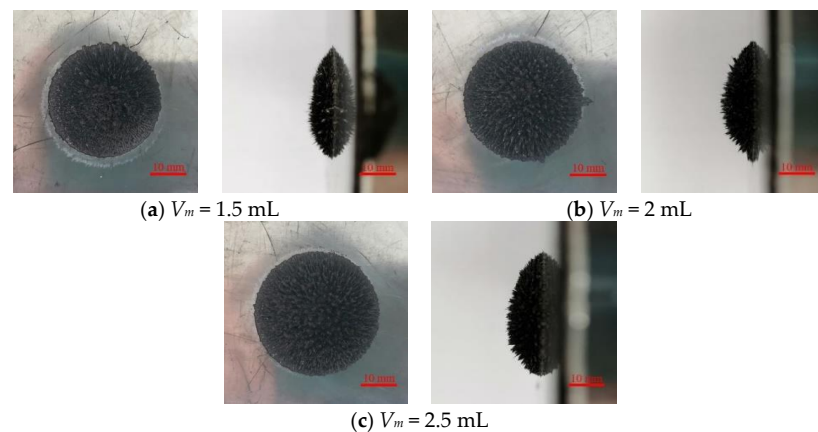


Figure 7. The final appearances of MCF tools with different MCF supplies under eccentricity of 4 mm.

In order to investigate thoroughly, a simplified schematic, as shown in Figure 8, was obtained according to the appearances. Obviously, a lateral mountain shape with a circular base diameter of d and a maximum peak height of H_{max} is formed by the MCF slurry. As can be seen, the top of the mountain deviates significantly from the center of the bottom surface and rotates around the spindle of the magnet holder with the radius of L . According to the motion analysis, the larger the diameter of the base and the maximum height of the top, the greater the possibility of MCF slurry being spilled due to the centrifugal force generated by the MCF carrier rotation, and the more pronounced the top of the mountain's deviation from the center of the bottom surface, the lower the material removal at the center of the polishing region. Therefore, it is necessary to maintain the appropriate size of the MCF tool to obtain a better polishing effect.

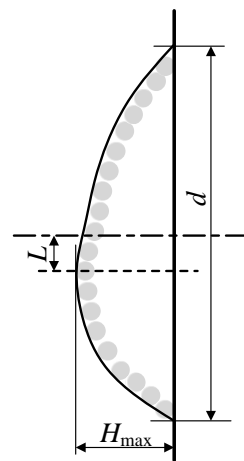


Figure 8. Schematic diagram of MCF tool.

Figure 9 analyzes the relationship between the eccentric distance r of the magnet and the morphology of the MCF slurry and the molding time T . It can be seen that the formation time T of the MCF tool decreases gradually with the increase in eccentricity r . When the eccentricity r increases from 2 to 4 mm, the formation time T of the MCF slurry decreases sharply. However, the decrease rate declines when the eccentricity r exceeds 4 mm. It is worth noting that when eccentricity $r = 0$ mm, eventually, a jagged MCF slurry is formed. Regarding the appearance of the MCF slurry, the MCF tool with a better appearance shape size is obtained at $r = 4$ mm. The value of circular base diameter d gradually increases as the eccentricity r increases, and the increasing tendency remains in a stable state. The maximum height H_{max} gradually decreases with the rise in eccentricity r , and its decrease tendency is basically the same as the increase in base diameter. The reason is that the MCF slurry supply remains constant, and the maximum height and the base diameter's

changing trends are opposite. Moreover, the distance L between the maximum height and the centerline decreases first and then increases with the increase in eccentricity r , and the value of L reaches the minimum at $r = 4$ mm.

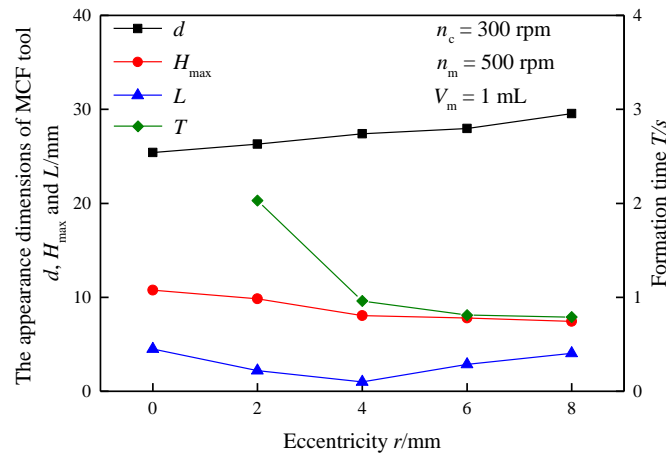


Figure 9. The influence of eccentric distance r on the shape size and formation time T of MCF tool.

The influence of the MCF slurry supply on the geometric size and formation time T of the MCF tool are shown in Figure 10. The values of the base diameter d , the maximum height H_{max} , the distance L between the maximum height and the centerline, and the formation time T all grow with the increase in the MCF slurry supply, and the growth rate is consistent. The reason is that the MCF slurry supply has increased, resulting in an increasing number of magnetic clusters. However, the MCF slurry becomes easier to dislodge from the polishing area as the slurry driven by the rotary carrier is uncontrolled with the increase in MCF supply. Therefore, when the volume of MCF slurry is 1 mL, the best morphology is obtained.

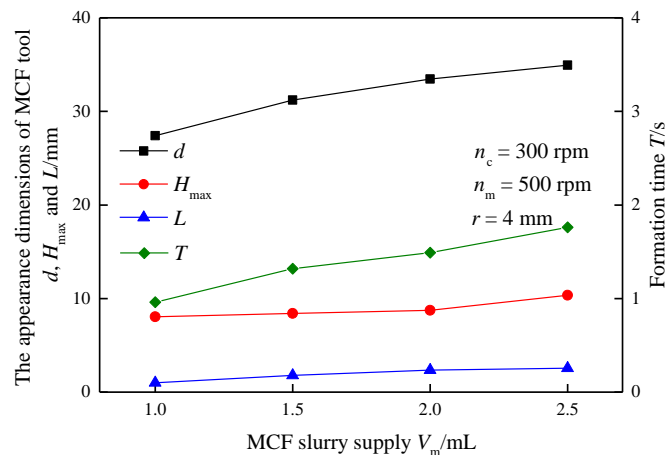


Figure 10. The effects of MCF slurry supply on the appearance dimensions and formation time T of MCF tool.

In addition, according to previous studies, the effects of the rotation speed of the magnet n_m and the rotation speed of the MCF carrier n_c on the appearance of the MCF tool are negligible [41]. In conclusion, when the eccentric distance r is 4 mm and the supply of MCF slurry is 1 mL, the MCF polishing tool is the best.

3.2. Optimal Processing Parameters

Before formally using the device for MCF polishing, it is necessary to decide the optimal parameters. Therefore, a multi-factor and multi-level orthogonal experiment is designed and carried out to explore the optimal parameters of the device. In addition,

by comparing the best surface roughness R_a and MRR, the relationship between process parameters and polishing effect is analyzed. It is found during the measurements that the optimal surface roughness is primarily found in the shaded area shown in Figure 11. This part will be further explored in future studies. Meanwhile, the previous study found that an annular polishing area with a W-shaped cross-section was generated, shown in Figure 12a [28]. Therefore, the maximum material removal depth MR_{max} was used to characterize the material removal during MCF polishing.

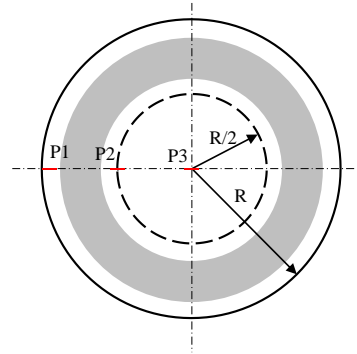


Figure 11. Schematic diagram of measuring points in the polishing area.

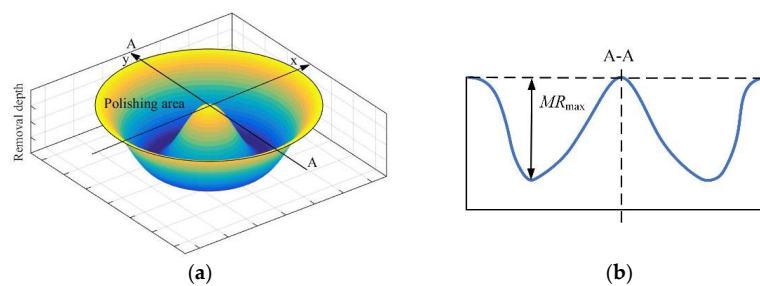


Figure 12. Features of the polishing area: (a) a 3D profile of the polishing area, (b) A-A cross-sectional profile.

According to the study described in Section 2.1, the eccentricity, machining gap, MCF carrier speed, and magnet speed have great influences on the polishing effect. It was found that if the machining gap was too small or the carrier speed was too large, the liquid within the MCF slurry would splash during the polishing process. Therefore, the levels of process parameters were designed as shown in Table 3.

Table 3. Process parameters and their levels.

Level	Eccentricity r/mm	Machining Gap Δ/mm	Rotation Speed of the MCF Carrier n_c/rpm	Rotation Speed of the Magnet n_m/rpm
1	2	1	200	300
2	4	1.5	300	400
3	6	2	400	500
4	8	2.5	500	600

The results of the orthogonal experiment are shown in Table 4. In this study, 16 groups of process tests were completed. The surface roughness R_a before and after MCF polishing was measured, and the maximum material removal depth of each sample was recorded. Since the surface roughness of each workpiece before polishing is different, in order to better represent the polishing effect of the workpiece, the surface roughness reduction rate $Ra\%$ is used to explain.

$$Ra\% = \frac{Ra_i - Ra_p}{Ra_i} \times 100\% \quad (17)$$

where Ra_i is the surface roughness before polishing, and Ra_p is the surface roughness after polishing.

Table 4. Plan of experiments and the responses obtained.

Test No.	r/mm	Δ/mm	n_c/rpm	n_m/rpm	$Ra_i/\mu\text{m}$	$Ra_p/\mu\text{m}$	$Ra\%$	$MR_{max}/\mu\text{m}$
1	2	1	200	300	0.409	0.028	93.154	11.279
2	2	1.5	300	400	0.467	0.032	93.147	9.822
3	2	2	400	500	0.408	0.069	83.088	8.724
4	2	2.5	500	600	0.523	0.123	76.482	8.618
5	4	1	300	500	0.373	0.010	97.319	15.732
6	4	1.5	200	600	0.383	0.031	91.906	10.732
7	4	2	500	300	0.497	0.080	83.903	13.745
8	4	2.5	400	400	0.461	0.120	73.970	7.814
9	6	1	400	600	0.406	0.026	93.596	15.917
10	6	1.5	500	500	0.420	0.016	96.190	12.334
11	6	2	200	400	0.429	0.163	62.005	10.652
12	6	2.5	300	300	0.387	0.190	50.904	6.974
13	8	1	500	400	0.496	0.010	97.984	12.764
14	8	1.5	400	300	0.425	0.019	95.529	8.015
15	8	2	300	600	0.386	0.103	73.316	7.307
16	8	2.5	200	500	0.466	0.218	53.219	6.938

The results of the orthogonal test are analyzed as shown in Table 5. K_i ($i = 1, 2, 3, 4$) is the mean value of the surface roughness decrease rate for each parameter at different levels, and F_i ($i = 1, 2, 3, 4$) is the mean value of the maximum material removal depth for each parameter at different levels. R and T are the range; if the range of a certain parameter is more prominent, it means that the influence of this parameter on the experimental results is more remarkable.

Table 5. Analysis of experimental results.

	r/mm	Δ/mm	n_c/rpm	n_m/rpm
K_1	86.468	95.513	75.071	80.873
K_2	86.775	94.193	78.672	81.777
K_3	75.674	75.578	86.546	82.454
K_4	80.012	63.644	88.640	83.825
R	11.101	31.869	13.569	2.952
F_1	9.61	13.923	9.9	10.003
F_2	12.005	10.226	9.959	10.263
F_3	11.469	10.014	10.117	10.931
F_4	8.756	7.585	11.865	10.643
T	3.249	6.338	1.965	0.928

The mean value of the surface roughness decrease rate $Ra\%$ at different levels of various parameters is shown in Figure 13. The decrease rate reaches the maximum value when the eccentricity r , machining gap Δ , the rotation speed of the magnet n_m , and the rotation speed of the MCF carrier n_c are 4 mm, 1 mL, 600 rpm, and 500 rpm, respectively. With the increase in eccentric distance, the decline first increases and then decreases, and reaches the maximum when the eccentricity is 4 mm, which is consistent with the result that the apparent shape of the MCF tool is the most ideal when the eccentricity is 4 mm. In addition, the decrease rate also declines with the increase in the machining gap, and grows with the growth of the rotational speed of the MCF carrier plate and the magnet. According to the definition of decrease rate $Ra\%$, the $Ra\%$ can represent the overall polishing effect of the workpiece. Therefore, when the eccentric distance r , machining gap Δ , magnet speed n_m , and MCF carrier speed n_c are 4 mm, 1 mL, 600 rpm, and 500 rpm, the resulting surface quality is the best.

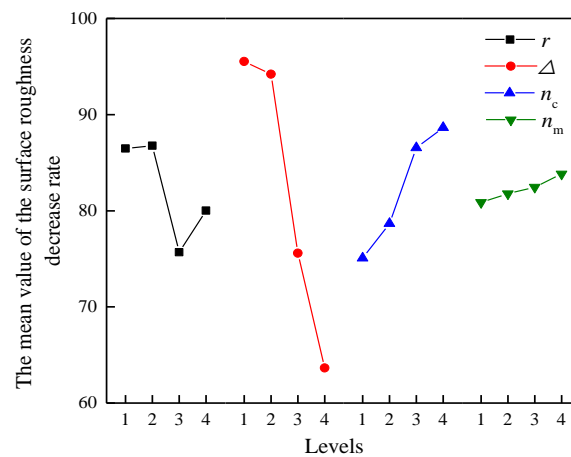


Figure 13. The mean value of the surface roughness decrease rate at different levels of various parameters.

Meanwhile, it should be noted from Figure 13 that the machining gap has the greatest impact on surface roughness, followed by the speed of the MCF carrier. The machining gap affects the magnetic field intensity in the machining area, which affects the polishing force of the abrasive grains in the polishing fluid. The rotational speed of the MCF carrier affects the velocity of the abrasive grains relative to the workpiece surface. The larger the relative speed is, the more the abrasive grains participate in cutting at the same time.

The mean value of the maximum material removal depth MR_{max} at different levels of various parameters is shown in Figure 14. It has a trend consistent with the decline rate of surface roughness. However, MR_{max} reaches the maximum value when the rotation speed of the magnet is 500 rpm, which is different from Figure 13. The reason is that the stirring effect of the magnetic lines of force is too strong for the MCF slurry due to the excessive rotation of the magnet. The contact time of the abrasive grains with the workpiece surface is too short to utilize the micro-cutting effect of the abrasive grain fully. Therefore, the maximum amount of material removal was obtained when the eccentricity r , the machining gap Δ , the magnet speed n_m , and the MCF carrier n_c speed were 4 mm, 1 mL, 500 rpm, and 500 rpm, respectively.

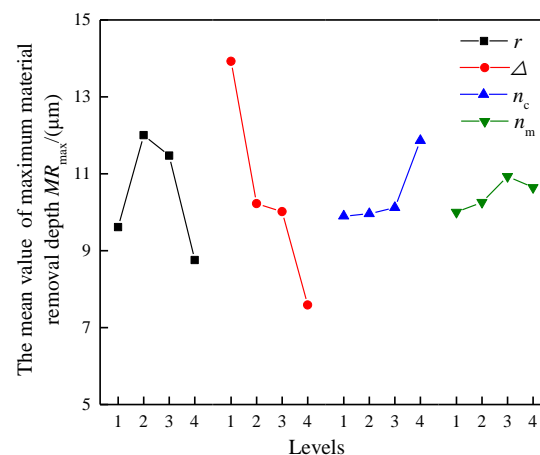


Figure 14. The mean value of the maximum material removal depth at different levels of various parameters.

At the same time, comparing the effects of various process parameters on the maximum material removal depth, it can be found that the influence of the magnet speed on material removal is minimal. Moreover, the maximum material removal depth when the rotation speed of the magnet is 600 rpm is second only to that when the rotation speed of the magnet is 500 rpm.

In addition, considering Figures 13 and 14 comprehensively, the influence of the processing parameters on surface roughness is more significant than that on material

removal. Therefore, when the eccentricity distance r is 4 mm, the machining gap Δ is 1 mm, the magnet speed n_m is 600 rpm, and the MCF carrier speed n_c is 500 rpm, the best polishing effect is obtained.

3.3. MCF Service Life

In order to inhibit the drying of the MCF slurry and prolong its service time, the following experiments were designed. The workpiece was polished for 10 min under the condition of no addition, and then the workpiece was replaced without changing the MCF slurry, and the process was continued for 10 min. The above steps were repeated until the accumulated processing time was 60 min. The weight change of the MCF slurry before and after the polishing was also measured to determine the water loss during the polishing process. At the same time, in order to explore whether there were other losses besides water in the polishing process, MF was also added as the control (using a syringe for addition). It was determined that the weight of the MCF slurry decreased by 0.724 g after polishing for 60 min. Therefore, 0.1 mL water or MF should be added to the MCF slurry every 10 min.

The optimal surface roughness of the polishing area under different addition conditions and its decrease rate are shown in Figure 15. Regardless of the addition conditions, the decrease rate shows a declining trend. The decrease rate with no addition was reduced more dramatically, while the decrease rate when adding water and MF recovered slightly after a sharp decline. The decrease rate is more significant when adding MF compared with adding water. The reason is that due to the addition of MF, the viscosity of the MCF slurry becomes larger, which leads to a more significant polishing force.

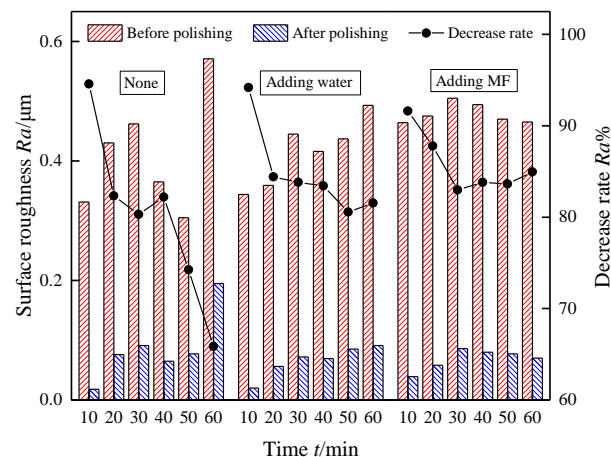


Figure 15. The optimal surface roughness of the polishing area under different supplementary conditions and its decrease rate.

In order to better represent the surface roughness of the polishing area, different positions of the polishing area (P1, P2, P3) were measured, as shown in Figure 11. Furthermore, the obtained data samples were statistically analyzed, and the overall surface roughness decrease rate of the polishing area was expressed in the form of error bars, as shown in Figure 16. In this experiment, the values of material removal at point P1 and P3 are far lower than that of P2, which result in large differences in the surface roughness in different areas. Consequently, the range of error bars in the decrease rate of surface roughness is wide, which is shown in the figure. Overall, the decrease rate is the largest when MF is added, followed by the decrease rate when water is added, and the decrease rate is the smallest with no addition.

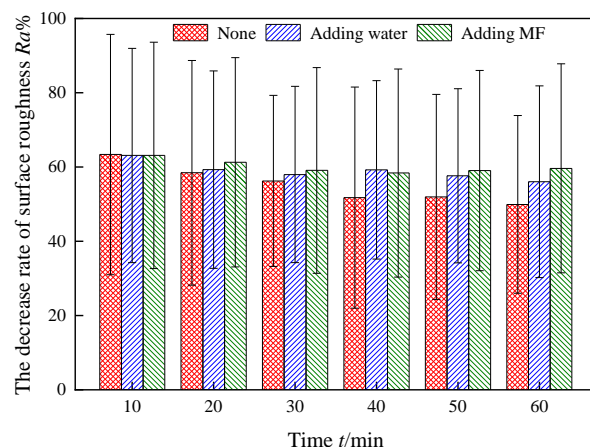


Figure 16. The decreased rate of surface roughness in the polishing area.

The material removal rate of the polishing area under different addition conditions is shown in Figure 17. When no water and MF are supplied (“None”), the material removal ability is significantly reduced after 60 min of polishing. However, when water and MF are provided, the material removal rate is significantly improved compared to the former condition. The material removal rate is the largest when MF is added, and the processing performance of the MCF slurry can best be maintained in this case.

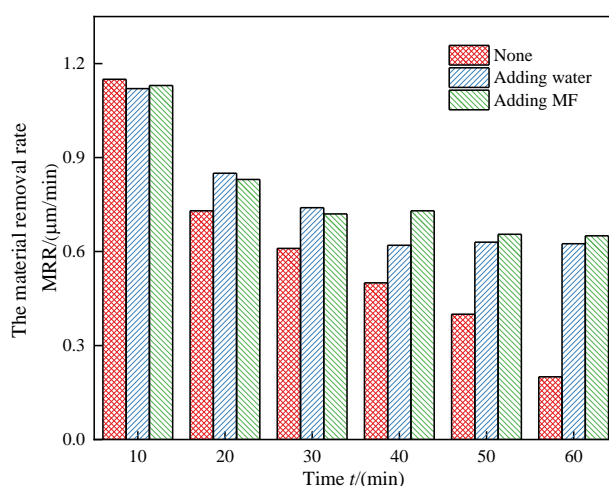


Figure 17. Material removal rate under different supplementary conditions.

4. Conclusions

In order to solve the water loss problem of MCF slurry during the experiment, an experimental setup was built to add water or MF into the MCF slurry conveniently. The appearance morphology and forming time of the MCF tool were observed. The orthogonal experiments were designed to determine the optimal process parameters of the polishing device. Finally, the polishing experiment of adding water or MF to the MCF slurry was carried out under the optimal processing parameters, which confirmed the feasibility of this polishing device to extend the service life of the MCF slurry and reduce the production and processing costs by adding water or MF, which is of great significance in production and application. The results are analyzed as follows.

- (1) The MCF polishing tool has the best polishing effect when the eccentricity r and MCF slurry supply V are 4 mm and 1 mL.
- (2) The formation time of the MCF tool decreased sharply when the eccentricity increased from 2 to 4 mm, but once the eccentricity exceeded 4 mm, the trend of decline became reversed. Moreover, with the increase in supply, the formation time grew steadily.

- (3) An ideal processing result could be obtained when the machining gap Δ , the revolution speed of the MCF carrier n_c , the eccentricity r , and the revolution speed of the magnet n_m were 1 mm, 500 rpm, 4 mm, and 600 rpm, respectively. Moreover, the influence of the processing parameters on surface roughness is more significant than that on material removal.
- (4) Adding water and MF could extend the service life of MCF, and, compared with adding water, adding MF could obtain a better polishing effect.

Author Contributions: Conceptualization, Y.W. and X.G.; methodology, Y.W.; software, X.G.; validation, J.G. and X.G.; formal analysis, M.F.; investigation, X.C. and W.Z.; resources, Y.W. and M.F.; data curation, X.G. and J.G.; writing—original draft preparation, Y.W.; writing—review and editing, Y.W., X.G., and J.G.; visualization, X.C.; supervision, W.Z. and Y.W.; project administration, Y.W. and X.C.; funding acquisition, Y.W. All authors have read and agreed to the published version of the manuscript.

Funding: The project is supported by the National Natural Science Foundation of China (No. 52265056), Gansu Provincial Fund (21JR7RA228), Hongliu Youth Fund of Lanzhou University of Technology (No. 07/062004), Young Doctor Fund of Higher Education Institutions in Gansu Province (2021QB-048), Natural Science Foundation of Zhejiang Province (CN) (No. LQ22E050008) and Natural Science Foundation of Wenzhou City (CN) (Grant No. G20210001).

Data Availability Statement: The study did not report any data.

Conflicts of Interest: The authors declare that they have no conflict of interest.

Abbreviations

Magnetic compound fluid	MCF
Magnetic fluid	MF
Magnetorheological	MR
Carbonyl iron particles	CIPs
Material removal rate	MRR
Eccentricity distance	r
Machining gap	Δ
Supplying of MCF slurry	V
Polishing time	t
The rotation speed of the MCF carrier	n_c
The rotation speed of the magnet	n_m
Surface roughness reduction rate	$Ra\%$
Maximum material removal depth	MR_{max}
Surface roughness before polishing	Ra_i
Surface roughness after polishing	Ra_p
Magnetic levitation force	F_{abr}
Volume of abrasive grains	V_{abr}
Permeability of vacuum	μ_0
Intensity of magnetization	M_f
Gradient of the magnetic field	∇H
Magnetization of iron powder	M
Permeability of the magnetic particle	μ
Magnetic field intensity	H
Volume ratio of magnetic particles	φ
Brinell hardness	H_B
Diameter of the abrasive grain	D_{abr}
Pressure of the abrasive grain	P
Depth of abrasive embedding	h

References

1. Li, M.; Yuan, J.L.; Wu, Z. Progress in ultra-precision machining methods of complex curved parts. *J. Mech. Eng.* **2015**, *51*, 178–191. [\[CrossRef\]](#)
2. Yuan, J.L.; Zhang, F.; Dai, Y.; Kang, R.; Yuan, H.; Lv, B. Development research of science and technologies in ultra-precision machining field. *J. Mech. Eng.* **2010**, *46*, 161–177. [\[CrossRef\]](#)
3. Guo, D.; Sun, Y.; Jia, Z. Methods and research progress of high performance manufacturing. *J. Mech. Eng.* **2014**, *50*, 119–134. [\[CrossRef\]](#)
4. Li, M.; Karpuschewski, B.; Ohmori, H.; Riemer, O.; Wang, Y.; Dong, T. Adaptive shearing-gradient thickening polishing (AS-GTP) and subsurface damage inhibition. *Int. J. Mach. Tools Manuf.* **2021**, *160*, 103651. [\[CrossRef\]](#)
5. Houshi, M.N. A comprehensive review on magnetic abrasive finishing process. *Adv. Eng. Forum* **2016**, *18*, 1–20. [\[CrossRef\]](#)
6. Yin, S. *Ultra-Precision Finishing Technology Assisted by Magnetic Field*, 1st ed.; Hunan University Press: Changsha, China, 2009; pp. 163–179.
7. Li, M.; Song, F.; Huang, Z. Control strategy of machining efficiency and accuracy in weak-chemical-coordinated-thickening polishing (WCCTP) process on spherical curved 9Cr18 components. *J. Manuf. Process.* **2022**, *74*, 266–282. [\[CrossRef\]](#)
8. Cheng, Q.; Fan, Z.; Tian, Y.; Liu, Y.; Han, J.; Wang, J. A review on magnetic abrasive finishing. *Int. J. Adv. Manuf. Technol.* **2020**, *112*, 619–634.
9. Kumari, C.; Chak, S. A review on magnetically assisted abrasive finishing and their critical process parameters. *Manuf. Rev.* **2018**, *5*, 13. [\[CrossRef\]](#)
10. Jiang, F.; Yan, L.; Huang, Y.; Xu, X. Review on magnetic field assisted machining technology. *J. Mech. Eng.* **2016**, *52*, 1–9. [\[CrossRef\]](#)
11. Li, M.; Xie, J. Green-chemical-jump-thickening polishing for silicon carbide. *Ceram. Int.* **2022**, *48*, 1107–1124. [\[CrossRef\]](#)
12. Yuan, J.; Wu, Z.; Lv, B.; Nguyen, D.; Lu, H.; Zhao, P. Review on ultra-precision polishing technology of aspheric surface. *J. Mech. Eng.* **2012**, *48*, 167–177. [\[CrossRef\]](#)
13. Tani, Y.; Kawata, K.; Nakayama, K. Development of high-efficient fine finishing process using magnetic fluid. *CIRP Ann. Manuf. Technol.* **1984**, *33*, 217–220. [\[CrossRef\]](#)
14. Yin, S.; Xu, Z.; Duan, H.; Chen, F. Effects of magnetic fluid on machining characteristics in magnetic field assisted polishing process. *Adv. Mater. Res.* **2013**, *797*, 396–400. [\[CrossRef\]](#)
15. Liu, T. *Study on Synthesis of Magnetic Fluids Containing Carbon Coated Fe and Fe-Ni Nanoparticles*, 1st ed.; China University Mining and Technology Press: Xuzhou, China, 2008; pp. 21–32.
16. Kordonski, W.; Golini, D. Progress update in magnetorheological finishing. *Int. J. Mod. Phys. B* **1999**, *13*, 2205–2212. [\[CrossRef\]](#)
17. Wang, J.; Xiao, Q. Research progress of magnetorheological polishing technology. *Surf. Technol.* **2019**, *48*, 317–328.
18. Jacobs, S.; Arrasmith, S.; Kozhinova, I.; Gregg, L.; Hogen, S. An overview of magnetorheological finishing (MRF) for precision optics manufacturing. *Ceram. Trans.* **1999**, *102*, 185–199.
19. Jha, S.; Jain, V. Design and development of the magnetorheological abrasive flow finishing (MRAFF) process. *Int. J. Mach. Tools Manuf.* **2004**, *44*, 1019–1029. [\[CrossRef\]](#)
20. Das, M.; Jain, V.; Ghoshdastidar, P. Fluid flow analysis of magnetorheological abrasive flow finishing (MRAFF) process. *Int. J. Mach. Tools Manuf.* **2007**, *48*, 415–426. [\[CrossRef\]](#)
21. Jha, S.; Jain, V. Modeling and simulation of surface roughness in magnetorheological abrasive flow finishing (MRAFF) process. *Wear* **2006**, *261*, 856–866. [\[CrossRef\]](#)
22. Zhang, F.; Wang, H.; Luan, D. Research on machining mechanics and experiment of ultrasonic-magnetorheological compound finishing. *Int. J. Comput. Appl. Technol.* **2007**, *29*, 252–256. [\[CrossRef\]](#)
23. Wang, H.; Zhang, F.; Zhang, Y.; Luan, D. Research on material removal of ultrasonic-magnetorheological compound finishing. *Int. J. Mach. Mach. Mater.* **2007**, *2*, 50–58. [\[CrossRef\]](#)
24. Shimada, K.; Akagami, Y.; Kamiyama, S.; Fujita, T.; Shibayama, A. New microscopic polishing with magnetic compound fluid (MCF). *J. Intell. Mater. Syst. Struct.* **2002**, *13*, 405–408. [\[CrossRef\]](#)
25. Shimada, K.; Fujita, T.; Oka, H.; Akagami, Y.; Kamiyama, S. Hydrodynamic and magnetized characteristics of MCF (magnetic compound fluid). *Trans. Jpn. Soc. Mech. Eng.* **2001**, *67*, 3034–3040. [\[CrossRef\]](#)
26. Wang, Y.; Wu, Y.; Nomura, M. Feasibility study on surface finishing of miniature V-grooves with magnetic compound fluid slurry. *Precis. Eng.* **2016**, *45*, 67–78. [\[CrossRef\]](#)
27. Wang, Y.; Wu, Y.; Nomura, M. Fundamental investigation on nano-precision surface finishing of electroless Ni–P-plated STAVAX steel using magnetic compound fluid slurry. *Precis. Eng.* **2017**, *48*, 32–44. [\[CrossRef\]](#)
28. Shimada, K.; Wu, Y.; Matsuo, Y.; Yamamoto, K. Float polishing technique using new tool consisting of micro magnetic clusters. *J. Mater. Process. Technol.* **2005**, *162*, 690–695. [\[CrossRef\]](#)
29. Furuya, T.; Wu, Y.; Nomura, M.; Shimada, K.; Yamamoto, K. Fundamental performance of magnetic compound fluid polishing liquid in contact-free polishing of metal surface. *J. Mater. Process. Technol.* **2007**, *201*, 536–541. [\[CrossRef\]](#)
30. Wu, Y.; Sato, T.; Lin, W.; Yamamoto, K.; Shimada, K. Mirror surface finishing of acrylic resin using MCF-based polishing liquid. *Int. J. Abras. Technol.* **2010**, *3*, 11–24. [\[CrossRef\]](#)
31. Guo, H.; Wu, Y.; Lu, D.; Fujimoto, M.; Nomura, M. Effects of pressure and shear stress on material removal rate in ultra-fine polishing of optical glass with magnetic compound fluid slurry. *J. Mater. Process. Technol.* **2014**, *214*, 2759–2769. [\[CrossRef\]](#)

32. Sato, T.; Wu, Y.; Lin, W.; Shimada, K. Study on magnetic compound fluid (MCF) polishing process using fluctuating magnetic field. *Trans. Jpn. Soc. Mech. Eng.* **2009**, *75*, 1007–1012. [[CrossRef](#)]
33. Sato, T.; Wu, Y.; Lin, W.; Shimada, K. Study of three-dimensional polishing using magnetic compound fluid (MCF). *Adv. Mater. Res.* **2009**, *849*, 288–293. [[CrossRef](#)]
34. Nomura, M.; Makita, N.; Fujii, T.; Wu, Y. Effects of water supply using ultrasonic atomization on the working life of MCF slurry in MCF polishing. *Int. J. Autom. Technol.* **2019**, *13*, 743–748. [[CrossRef](#)]
35. Shorey, A.; Jacobs, S.; Kordonski, W.; Gans, R. Experiments and observations regarding the mechanisms of glass removal in magnetorheological finishing. *Appl. Opt.* **2001**, *40*, 20–33. [[CrossRef](#)] [[PubMed](#)]
36. Kim, D.; Cho, M.; Seo, T.; Shin, Y. Experimental Study on the Effects of Alumina Abrasive Particle Behavior in MR Polishing for MEMS Applications. *Sensors* **2008**, *8*, 222–235. [[CrossRef](#)] [[PubMed](#)]
37. Sidpara, A.; Jain, V. Analysis of forces on the freeform surface in magnetorheological fluid based finishing process. *Int. J. Mach. Tools Manuf.* **2013**, *69*, 1–10. [[CrossRef](#)]
38. Sidpara, A.; Jain, V. Theoretical analysis of forces in magnetorheological fluid based finishing process. *Int. J. Mech. Sci.* **2012**, *56*, 50–59. [[CrossRef](#)]
39. Liang, H.; Yan, Q.L.; Lu, J.; Luo, B.; Xiao, X. Material removal mechanisms in chemical-magnetorheological compound finishing. *Int. J. Adv. Manuf. Technol.* **2019**, *103*, 1337–1348. [[CrossRef](#)]
40. Peng, X.; Dai, Y.; Li, S. Mathematical model of material removal in magnetorheological polishing. *J. Mech. Eng.* **2004**, *40*, 67–70. [[CrossRef](#)]
41. Pawan, P.; Jain, K. Computational simulation of abrasive flow machining for two dimensional models. *Mater. Today: Proc.* **2018**, *5*, 12969–12983.
42. Peng, Z.; Song, W.; Ye, C.; Shi, P.; Choi, S. Model establishment of surface roughness and experimental investigation on magnetorheological finishing for polishing the internal surface of titanium alloy tubes. *J. Intell. Mater. Syst. Struct.* **2021**, *32*, 1278–1289. [[CrossRef](#)]
43. Jain, R.; Jain, V.; Dixit, P. Modeling of material removal and surface roughness in abrasive flow machining process. *Int. J. Mach. Tools Manuf.* **1999**, *39*, 1903–1923. [[CrossRef](#)]
44. Guo, H.; Wu, Y. Behaviors of MCF (magnetic compound fluid) slurry and its mechanical characteristics: Normal and shearing forces under a dynamic magnetic field. *J. Jpn. Soc. Exp. Mech.* **2012**, *12*, 369–374.